Contrib Mineral Petrol (2004) 147: 740–749
DOI 10.1007/s00410-004-0588-9

ORIGINAL PAPER

P. Tropper · C. E. Manning

Paragonite stability at 700°C in the presence of H_2O–NaCl fluids: constraints on H_2O activity and implications for high pressure metamorphism

Received: 5 November 2003 / Accepted: 28 April 2004 / Published online: 9 July 2004

Abstract We carried out reversed piston-cylinder experiments on the equilibrium paragonite = jadeite + kyanite + H_2O at 700°C, 1.5–2.5 GPa, in the presence of H_2O-NaCl fluids. Synthetic paragonite and jadeite and natural kyanite were used as starting materials. The experiments were performed on four different nominal starting compositions: $X(H_2O) = 1.0$, 0.90, 0.75 and 0.62. Reaction direction and extent were determined from the weight change in H_2O in the capsule, as well as by optical and scanning electron microscopy (SEM). At $X(H_2O) = 1.0$, the equilibrium lies between 2.25 and 2.30 GPa, in good agreement with the 2.30–2.45 GPa reversal of Holland (Contrib Miner Petrol 68:293–301, 1979). Lowering $X(H_2O)$ decreases the pressure of paragonite breakdown to 2.10–2.20 GPa at $X(H_2O) = 0.90$ and 1.85–1.90 GPa at $X(H_2O) = 0.75$. The experiments at $X(H_2O) = 0.62$ yielded the assemblage albite + corundum at ≤ 1.60 GPa, and jadeite + kyanite at ≥ 1.70 GPa. This constrains the position of the isothermal paragonite–jadeite–kyanite–albite–corundum–H_2O invariant point in the system Na_2O–Al_2O_3–SiO_2–H_2O to be at 1.6–1.7 GPa and $X(H_2O) \sim 0.65 \pm 0.05$. The data indicate that H_2O activity, $a(H_2O)$, is 0.75–0.86, 0.55–0.58, and < 0.42 at $X(H_2O) = 0.90$, 0.75, and 0.62, respectively. These values approach $X(H_2O)^2$, and agree well with the $a(H_2O)$ model of Aranovich and Newton (Contrib Miner Petrol 125:200–212, 1996). Our results demonstrate that the presence or absence of paragonite can be used to place limits on $a(H_2O)$ in high-pressure metamorphic environments. For example, nearly pure jadeite and kyanite from a metapelite from the Sesia Lanzo Zone formed during the Eo-Alpine metamorphic event at 1.7–2.0 GPa, 550–650°C. The absence of paragonite requires a fluid with low $a(H_2O)$ of 0.3–0.6, which could be due to the presence of saline brines.

Introduction

Fluids play a fundamental role in subduction-zone processes (e.g., Philippot 1993; Iwamori 1998; Schmid and Poli 1998; Scambelluri and Philippot 2001; Ulmer 2001; Stern 2002; Jarrard 2003; Sadovsky and Bebout 2003; Manning 2004a). Although H_2O is typically the main solvent component, subduction-zone fluids from some environments may also contain significant concentrations of dissolved salts such as NaCl, KCl and $CaCl_2$ (e.g., Scambelluri and Philippot 2001; Touret 2001). For example, studies from the paleo-subduction zones of the Eastern and Western Alps, where significant continental subduction occurred, show that fluids contained elevated concentrations of salts (NaCl, $CaCl_2$, $MgCl_2$, KCl), as evidenced by fluid inclusions with up to 50 wt.% NaCl equivalent (Thomas 1991; Selverstone et al. 1992; Philippot and Selverstone 1991; Nadeau et al. 1993; Scambelluri and Philippot 2001). This contrasts with active and paleo-oceanic subduction margins, which show relatively low salinity of up to 7 wt.% NaCl equivalent (Fryer et al. 1990; Kimura et al. 1997; Giaramita and Sorensen 1994; Gao and Klemd 2001). As noted by Manning (2004a), the limited data evidently suggest that high salinities are found in environments in which continental subduction has occurred.

The chloride content of fluids plays an important role in mass transport and mineral-fluid-melt phase equilibria in geological environments (e.g., Yardley and Graham 2002). With respect to mass transport, high NaCl concentrations suppress quartz and albite solubility in H_2O–NaCl solutions at high pressure (Newton and

P. Tropper (✉)
Institute of Mineralogy and Petrography,
University of Innsbruck, Innrain 52,
6020 Innsbruck, Austria
E-mail: Peter.Tropper@uibk.ac.at

P. Tropper · C. E. Manning
Department of Earth and Space Sciences,
University of California, Los Angeles,
CA 90095-1567, USA
E-mail: Manning@ess.ucla.edu

Manning 2000; Shmulovich et al. 2001), but enhance the solubility of calcite and anhydrite (Newton and Manning 2002, 2004). These variations imply large changes in relative mineral solubilities with NaCl concentration. In addition, high salinity has been proposed as a mechanism for explaining the trace element abundances in arc magmas (Keppler 1996).

Although much attention has been focused on the effects of saline solutions on element solubility, there has been less consideration of the consequences for phase relations involving hydrous minerals in subduction-zone environments. High chloride concentrations reduce H_2O activity, which shifts the locations of dehydration and melting reactions. This will yield conditions of fluid and melt production different than if the fluid is nearly pure H_2O. Experimental study of these effects has been limited. Aranovich and Newton (1996, 1997) studied the brucite/periclase dehydration equilibrium in the presence of H_2O–NaCl and H_2O–KCl brines. They used this work to derive activity concentration relations in the brine systems which are experimentally constrained to 1.5 GPa. In addition, Aranovich and Newton (1998) examined the role of H_2O–KCl brines on the breakdown of phlogopite + quartz to form enstatite + K-feldspar + H_2O. However, there have been no experimental investigations on the mixing relations of H_2O–NaCl brines at higher pressure, or of the influence of brines on the stability limits of hydrous minerals relevant to subduction zones.

Paragonite is a widespread hydrous mineral in rocks from the blueschist and eclogite facies. It's stability depends strongly on H_2O activity. To assess this, we investigated the equilibrium

$$\begin{aligned}&\mathrm{NaAl_2Si_3AlO_{10}(OH)_2 = NaAlSi_2O_6 + Al_2SiO_5 + H_2O}\\&\text{Paragonite} = \text{Jadeite} + \text{Kyanite} + \mathrm{H_2O} \qquad (1)\end{aligned}$$

in the presence of of H_2O-NaCl brines. The purpose of this work was:(1) to determine the isothermal shift of the paragonite-breakdown reaction as a function of NaCl concentration, (2) to constrain $a(H_2O)$ for comparison with activity/composition relations of H_2O–NaCl brines at lower P (Aranovich and Newton 1996), and (3) to apply the experimental results to phase relations in jadeite + kyanite-bearing metapelites from the Sesia Lanzo Zone of the Western Alps.

Methods

Starting materials

Natural and synthetic minerals were used as starting materials. We used fired (950°C), natural kyanite from Brazil (0.15 wt% Fe_2O_3, Bohlen et al. 1991) and jadeite synthesized in a piston-cylinder apparatus. Paragonite was synthesized according to the technique of Holland (1979) by using jadeite glass which was then sealed with H_2O in a Pt capsule and run at 1.8 GPa at 650°C for 20 h. X-ray powder diffraction (Norelco-Philips vertical diffractometer, variable slit geometry) was used to verify the absence of additional phases.

Stoichiometric mixtures of the starting materials were ground together in a morter and pestle. Aliquots of this mixture (7 mg) were loaded with weighed amounts of halite (Fisher) and 1.5–2.0 mg H_2O into a Pt capsule (2 mm outer diameter) and sealed by arc welding. The experiments were carried out in the presence of fluids with four different nominal starting H_2O mole fractions $X(H_2O)$: 1.0, 0.90, 0.75 and 0.62.

Run procedures

All experiments were conducted in an end-loaded piston-cylinder apparatus similar to that described by Boyd and England (1960) with 25.4 mm (1 in.) diameter furnace assemblies and pistons. The furnace assembly is primarily made of graphite, NaCl and MgO (Bohlen 1984; Manning and Boettcher 1994). The capsule was placed horizontally in the graphite furnace and packed in boron nitride (BN) to reduce temperature gradients. A piece of Pt foil was placed on the top of the capsule to prevent puncture by the thermocouple. Temperature was measured with matched $Pt–Pt_{90}Rh_{10}$ thermocouples, with a precision estimated to be ± 3°C. Pressure was monitored using a HEISE gauge and the precision in pressure is about ± 0.01 GPa. The experiments were brought to final conditions using the piston-in method. First, a pressure of about two-thirds of the final value was applied. The temperature was then increased to the desired run temperature over a period of approximately 10 min. Finally the pressure was increased to the desired value. Run durations ranged from 38 to 94 h (Table 1).

After the experiments, the capsule was cleaned, pierced with a needle, dried at 115°C for 15 min and then at 400°C for 15 min. Since no water loss occurred during the experiments, comparison of water weights before and after experiments established reaction direction and extent. Increases in H_2O weight indicate H_2O release by paragonite breakdown, whereas decreases in H_2O weight indicate H_2O consumption by paragonite growth. Reaction direction and extent were also checked by optical and scanning electron microscope (SEM) petrography.

Analytical techniques

Quantitative analyses of paragonite from the run products were obtained with the JEOL 6310 SEM equipped with a LINK ISIS energy dispersive system and a MICROSPEC wavelength dispersive system at the Institute of Mineralogy and Petrology, University of Graz, Austria. The analytical conditions were 15 kV and 5 nA sample current. As standards we used synthetic quartz (Si), natural jadeite from Clear Creek, California (Na), synthetic corundum (Al) and natural atacamite (Cl). The elements Si, Al and Cl were analyzed with the

Table 1 Runtable of the experiments at 700°C

Run	GPa	Time (h)	H_2O (mg)	NaCl (mg)	$X(H_2O)$	Δ (H_2O)	Growth
$X(H_2O) = 1.0$							
Pg-4	2.20	41	2.058	–	1.00	−0.079	Pg
Pg-25	2.25	64	2.035	–	1.00	−0.036	Pg
Pg-6	2.30	50	2.056	–	1.00	+0.108	Jd + Ky
Pg-9	2.35	98	1.862	–	1.00	+0.181	Jd + Ky
Pg-5	2.45	41	1.915	–	1.00	+0.132	Jd + Ky
$X(H_2O) = 0.90$							
Pg-18	2.00	62	2.076	0.730	0.90	−0.024	Pg
Pg-24	2.10	67	1.983	0.762	0.89	−0.043	Pg
Pg-26	2.20	90	1.972	0.729	0.90	+0.099	Jd + Ky
Pg-20	2.25	94	2.005	0.722	0.90	+0.156	Jd + Ky
$X(H_2O) = 0.75$							
Pg-21	1.80	71	1.582	1.683	0.75	−0.422	Pg
Pg-27	1.85	56	1.542	1.644	0.75	−0.409	Pg
Pg-23	1.90	51	1.531	1.626	0.75	+0.029	Jd + Ky
Pg-17	2.00	62	1.567	1.659	0.75	+0.188	Jd + Ky
$X(H_2O) = 0.62$							
Pg-12	1.50	74	2.092	4.030	0.63	+0.008	Ab + Cor
Pg-10	1.60	74	2.059	4.027	0.62	+0.100	Ab + Cor
Pg-11	1.70	95	2.055	4.011	0.62	+0.128	Jd + Ky
Pg-8	1.80	38	2.144	4.058	0.63	+0.187	Jd + Ky
Pg-19	2.00	67	1.947	4.030	0.61	+0.142	Jd + Ky

$\Delta(H_2O)$ was obtained by determining the weight loss after heating the opened capsule after the experiments. The positive sign (increase in the amount of H_2O in the capsule during the experiments) indicates breakdown of paragonite and the negative sign (decrease in the amount of H_2O in the capsule during the experiments) indicates growth of paragonite. The last column indicates which phases increased in quantity during the experiments, but all experiments still contain to a variable extent the minerals from the starting assemblage

energy dispersive system and the Na-content was analyzed with the wavelength dispersive system, due to the better detection limit of 0.05–0.1 wt.% of the wavelength dispersive system.

Uncertainty in fluid composition

All weighings were made on a Mettler M3 microbalance. For this study, precision of individual weighings was estimated to be 0.004 mg at the 1σ level. Propagation of this weighing error yields 1σ in H_2O mole fraction of 0.0007. A larger source of uncertainty arises from minor evaporation of H_2O between loading into the capsule and welding. H_2O loss causes a slight increase in the nominal NaCl concentration. Our internal laboratory standardization of this shift suggests that the maximum H_2O lost to evaporation was 0.015 mg. This implies that H_2O mole fraction is accurate to at least ± 0.002.

Results

Experimental results are given in Table 1. The experiments yielded fine-grained experimental products. The stable assemblage was identified by gravimetry and textural observations. Weighing the capsules after experiments yielded a strong signal for reaction direction. The total amount of starting paragonite in the charges was 3.5 mg (0.0094 mole). Consumption of all paragonite would have led to an increase in the amount of H_2O by 0.17 mg. All jadeite + kyanite-producing experiments yielded H_2O weight gains of > 0.099 mg H_2O, indicating $> 58\%$ reaction by weight where paragonite is unstable. In three experiments (Pg-9, Pg-17, Pg-8), weight gains exceeded 0.17 mg (0.181–0.188 mg, Table 1). This could be due to: (1) excess H_3O^+ component in the synthetic paragonite, or (2) the presence of quench precipitates (Na–Si gel) which start to decompose during the drying process after puncturing the capsules. Consumption of H_2O during the runs in the paragonite stability field led to an increase in the amount of paragonite, ranging from 0.51 mg (1.3 μmol) in experiment Pg-18 to 8.95 mg (23 μmol) in experiment Pg-21.

The sign of the weight changes was consistent with reaction direction as indicated by textures. Paragonite growth (Fig. 1a) is characterized by a matrix of voluminous minute paragonite flakes, with minor relict embedded kyanite and/or jadeite crystals (Fig. 1a). By contrast, jadeite and kyanite newly grown via paragonite breakdown form subhedral to euhedral crystals with occasional recrystallization textures and development of newly formed crystal faces on crystals from the starting assemblage (Fig. 1b). In addition, no evidence of melting of the assemblage jadeite + paragonite + kyanite + H_2O was observed.

Weighing and textural observations established that, at $X(H_2O) = 1.0$, paragonite breaks down between 2.25 and 2.30 GPa (Fig. 2). Lowering $X(H_2O)$ yields a decrease in the pressure of paragonite breakdown to 2.10–2.20 GPa at $X(H_2O) = 0.90$ and 1.85–1.90 GPa at $X(H_2O) = 0.75$. At $X(H_2O) = 0.62 \pm 0.01$, paragonite breaks down to form the assemblage albite + corundum below 1.70 GPa, in the stability field of albite + corundum. Albite forms large crystals and corundum occurs as small plates interspersed with paragonite (Fig. 1c). Above 1.7 GPa, jadeite + kyanite form, occasionally pseudomorphing former paragonite crystals (Fig. 1d). This indicates that at < 1.7 GPa, $X(H_2O) = 0.62 \pm 0.01$, paragonite breaks down according to the reaction.

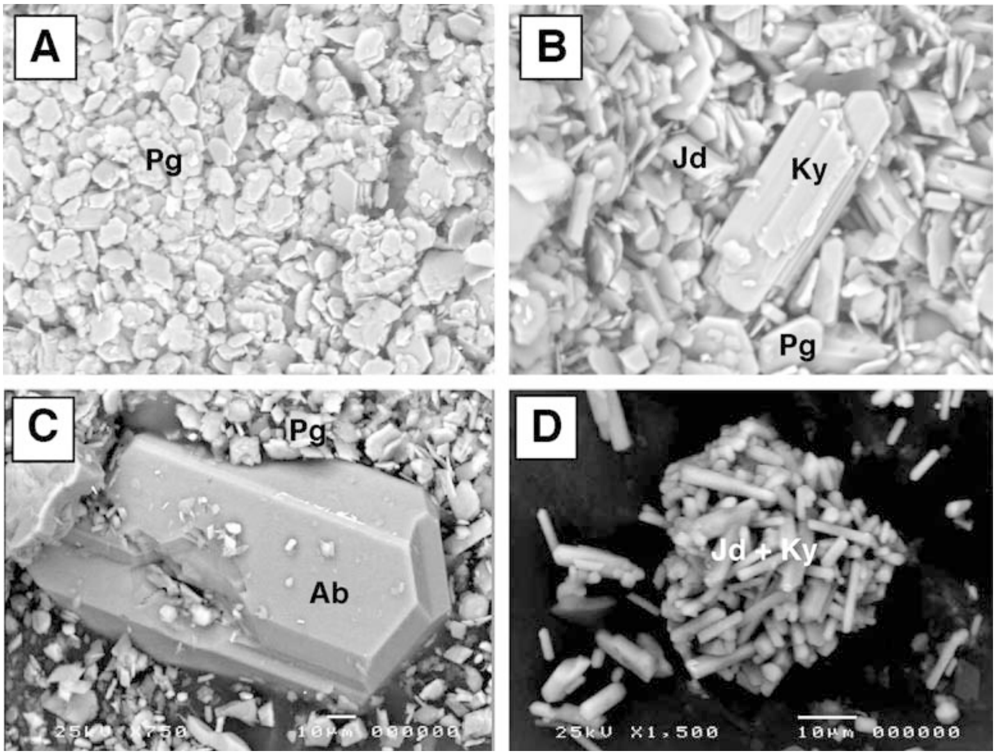

Fig. 1a–d Backscatter electron (BSE) images of the textural relations from the experiments. **a** textures from an experiment which were carried out in the paragonite stability field with $X(H_2O)$ of 1.0 (Pg-4). The starting assemblage has mostly been transformed into paragonite (Pg). **b** Texture from an experiment which was carried out in the jadeite (Jd) + kyanite (Ky) stability field with $X(H_2O)$ of 0.90 (Pg-20). In this experiment newly grown small jadeite and kyanite crystals occur. Kyanite also shows recrystallization and formation of newly grown crystal faces. **c** Texture from an experiment with $X(H_2O) = 0.62$, paragonite breaks down below 1.7 GPa to form the assemblage albite (Ab) + corundum and large albite crystals form (Pg-10). **d** Above 1.7 GPa, jadeite + kyanite form (Pg-11). All mineral abbreviations are according to Kretz (1983)

$$\begin{aligned} &NaAl_2Si_3AlO_{10}(OH)_2 = NaAlSi_3O_8 + Al_2O_5 + H_2O \\ &\text{Paragonite} = \text{Albite} + \text{Corundum} + H_2O \end{aligned} \tag{2}$$

The intersection of reactions 1 and 2 define an invariant point involving a third, H_2O-absent reaction:

$$\begin{aligned} &\text{Jadeite} + \text{Kyanite} \;=\; \text{Albite} + \text{Corundum} \\ &NaAlSi_2O_6 + Al_2SiO_5 = NaAlSi_3O_8 + Al_2O_5 \end{aligned} \tag{3}$$

Figure 2 shows a $P–X(H_2O)$ diagram with the schematic positions of these equilibria as inferred from the experimental observations.

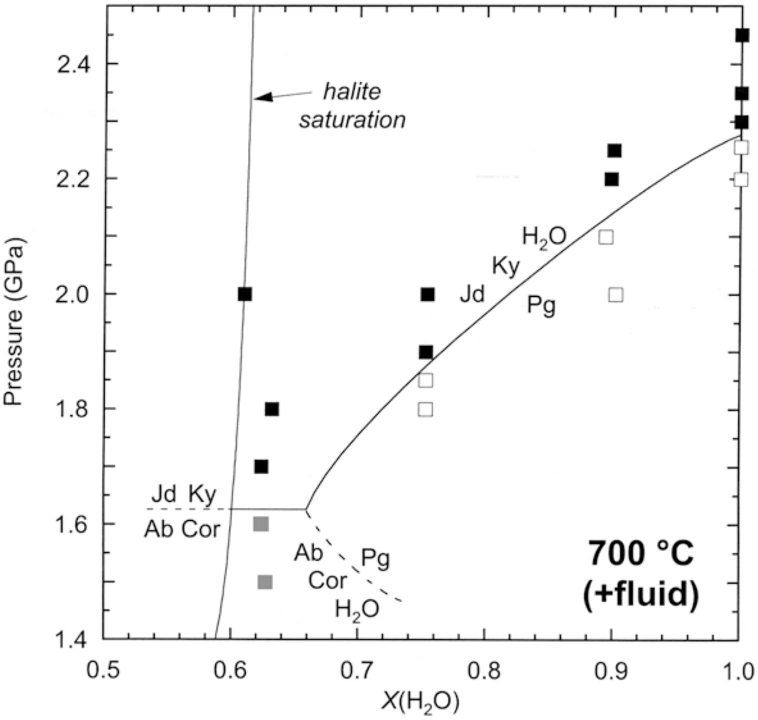

Fig. 2 $P–X(H_2O)$ diagram at 700°C with excess fluid, illustrating the experimental results and the schematic position of reactions 1, 2, 3 based on the observed phase relations. *Open squares* denote paragonite growth; *closed squares*, jadeite + kyanite growth; *shaded squares*, albite + corundum growth. Halite-saturation curve is extrapolated from Koster Van Groos (1991) and Aranovich and Newton (1996)

Table 2 Selected paragonite analyses from the experiments

	Pg-18	Pg-21
SiO_2	48.53	47.49
Al_2O_3	39.77	38.59
Na_2O	8.02	7.88
Cl	0.04	0.05
Total	96.35	94.01
Si	3.052	3.065
Al	2.948	2.935
Na	0.978	0.987
Cl	0.004	0.006
Σ cat.	6.978	6.987

The formulae were calcultaed on the basis of six cations + Na + K + Ca and 11 oxygens

Halite saturation defines the lowest $X(H_2O)$ attainable and has been been investigated at high P by Koster Van Groos (1991) and Aranovich and Newton (1996); however, both studies investigated pressures < 1.5 GPa. Consequently, the halite saturation curve was extrapolated to conditions of the present study (Fig. 2). Figure 2 shows that all experiments were conducted at $X(H_2O)$ > halite saturation. This is consistent with the absence of large, euhedral halite crystals in even the most NaCl-rich experiments (e.g., Pg-19, Table 1). Analyses of newly grown paragonite from two experiments (Pg-18, Pg-21) yield stoichiometric formulae with the sum of cations closely approaching a total of seven cations on a basis of 11 oxygens. Newly grown paragonite incorporated negligible Cl (≤ 0.05 wt.%, or 0.006 atoms per formula unit; Table 2).

Discussion

Comparison to previous results

Experimental investigations on reaction 1 were carried out by Holland (1979) in pure H_2O at 550–740°C. At 700°C, he obtained a reversal between 2.30 and 2.45 GPa. The present experiments locate the equilibrium to be between 2.25 and 2.30 GPa at $X(H_2O) = 1.0$ (Table 1, Fig. 2). This improves the precision for the stoichiometric reaction, while agreeing well with Holland's result.

Calculations from thermodynamic data show substantial variation in the computed position of reaction 1 at 700°C. The location calculated from SUPCRT92 (Johnson et al. 1992) yields 2.05 GPa. By contrast, calculations using Berman (1988, updated 1992) and Haar et al. (1984) give 2.40 GPa, whereas THERMOCALC v. 3.21 (R. Powell 2003, written communication) with the data base of Holland and Powell (1998) yields 2.32 GPa. The results of the present study suggest that Holland and Powell (1998) data most accurately predict the position of reaction 1. Accordingly, we used this dataset in all calculations that follow.

Table 3 Comparison of experimentally derived and calculated $a(H_2O)$ at 700°C

Bracketing experiment	P (GPa)	$a(H_2O)$		
		This study	Ideal fused-salt model	AN96 model
$X°_{NaCl} = 0.90$				
Pg-26	2.2	0.856	0.808	0.785
Pg-24	2.1	0.752	0.814	0.776
$X°_{NaCl} = 0.75$				
Pg-23	1.90	0.582	0.604	0.552
Pg-27	1.85	0.546	0.603	0.550
$X°_{NaCl} = 0.62$				
Pg-11	1.70	< 0.451	0.454	0.399
Pg-10	1.60	< 0.417	0.453	0.399

$X°_{NaCl}$ denotes nominal mole fraction of NaCl in experimental fluid; actual values vary slightly (Table 1). Activity of H_2O derived from experiments using THERMOCALC v. 3.21 (Holland and Powell 1998). The calculation of the activity of H_2O with the model of Aranovich and Newton (1996), AN96; the CORK equation of state for H_2O (Holland and Powell 1991) and the program RK (J. Connolly 2003, written communication) were used

Constraints on H_2O activity in H_2O–NaCl fluids at high pressure

Activity of H_2O, $a(H_2O)$, can be constrained by combining the new reversals at $X(H_2O) < 1.0$ with the calculated thermodynamic properties of reaction 1. At a given P and T, the equilibrium constant for reaction 1 corresponds to $a(H_2O)$, so the experimental brackets define maximum and minimum bounds on $a(H_2O)$. Values of $a(H_2O)$ derived from our experiments are less than $X(H_2O)$ (Table 3), and approach $X(H_2O)^2$.

As discussed by Aranovich and Newton (1996), $a(H_2O)$ values in H_2O-NaCl fluids at high P and T approximate those of an ideal fused-salt mixture, which can be expressed as:

$$a(H_2O) = X(H_2O)/2 - X(H_2O)) \tag{4}$$

Aranovich and Newton (1996) found that $a(H_2O)$ constrained by their experiments was lower than predicted by Eq. 4, which they interpreted to be the result of partial NaCl dissociation. To describe this they modified Eq. 4:

$$a(H_2O) = X(H_2O)/(1 + \alpha X(NaCl)) \tag{5}$$

where α is an empirical parameter describing extent of NaCl ionization as a function of P, T, and H_2O density. Aranovich and Newton (1996) experimentally calibrated Eq. 5 to a maximum of 1.5 GPa, and its extrapolability to higher P is uncertain.

Values of $a(H_2O)$ calculated using Eqs. 4 and 5 are compared to our experimental constraints in Table 3 and Fig. 3. The ideal fused-salt equation yields $a(H_2O)$ higher than those required by our reversals, in conjunction with the data of Holland and Powell (1998) as shown in Fig. 3a. In contrast, there is excellent agreement between the experimental results at 1.6–2.2 GPa

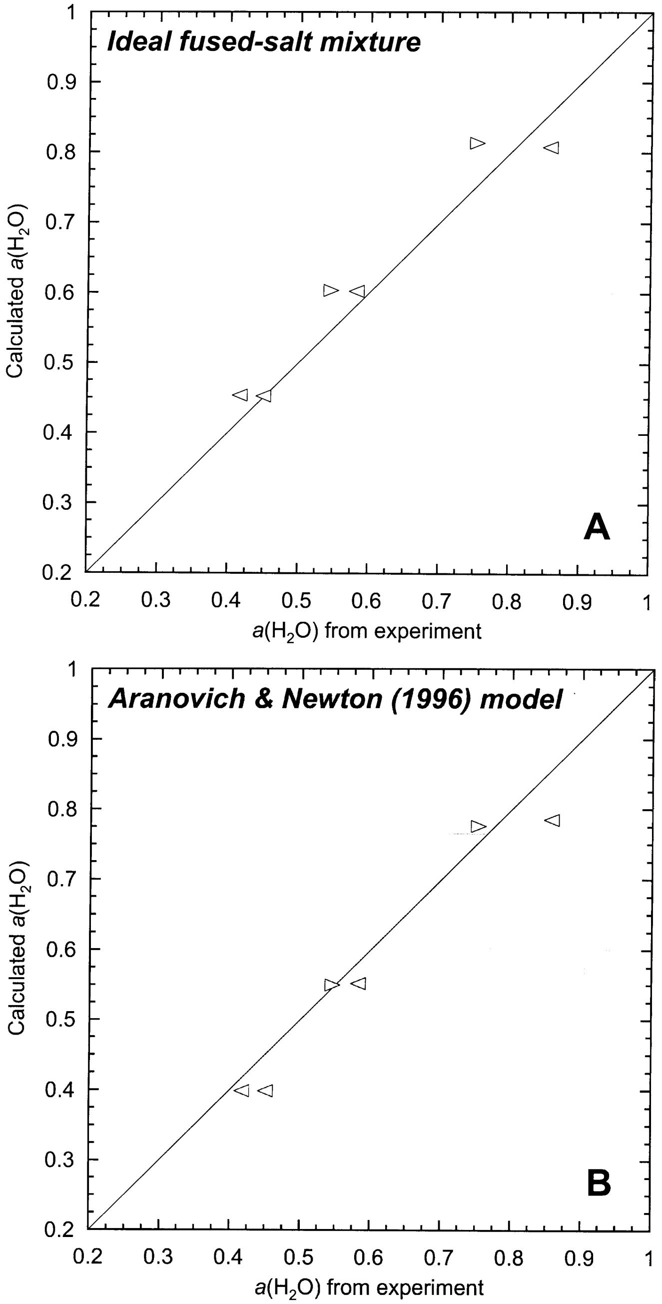

Fig. 3 Comparison of $a(H_2O)$ calculated from experimental brackets using THERMOCALC v. 3.21 (Holland and Powell 1998) with values computed from the model of Aranovich and Newton (1996) using $X(H_2O)$ in experimental fluids. The *line with unit slope* passes through the brackets, indicating that the Aranovich and Newton (1996) model can be successfully used to at least 2.0 GPa

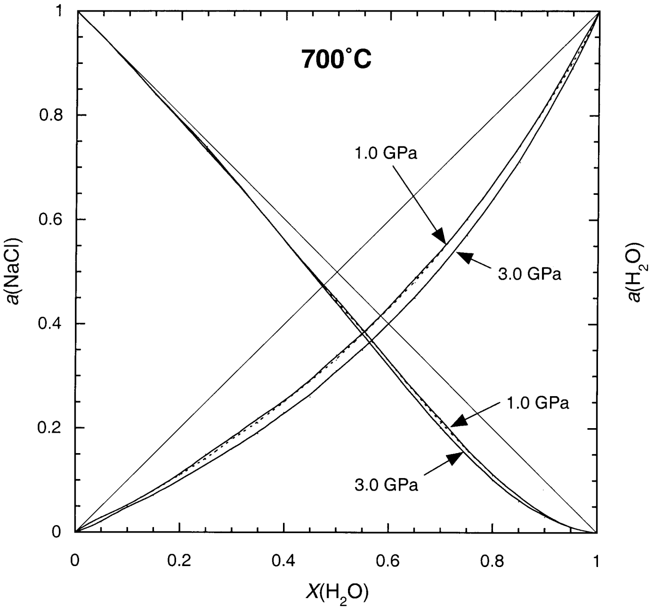

Fig. 4 a–X relations calculated for the system H_2O–NaCl at 700°C and pressures of 1.0 GPa and 3.0 GPa with the Aranovich and Newton (1996) model involving NaCl dissociation (*continuous line*) and the ideal fused-salt model (*stippled line*)

and the Aranovich and Newton (1996) model. These results suggest that the Aranovich and Newton (1996) model for H_2O–NaCl mixing is applicable to at least 2.0 GPa. Figure 4 shows the calculated a–X relations at 700°C and pressures ranging from 1.0 to 3.0 GPa. Predicted activity-composition relations exhibit very little dependence on P at >1 GPa, consistent with the steep slope of the halite-saturation curve in Fig. 2. This small dependence of $a(H_2O)$ on P explains in part the extrapolability of the model to high P.

Figure 5 gives experimental results and calculated positions of Eqs. 1, 2, and 3 as a function of $a(H_2O)$ and P. Values of $a(H_2O)$ for experiments were calculated using the Aranovich and Newton (1996) model. All results at $a(H_2O) < 1$ agree with calculated equilibria and the extrapolated halite-saturation curve (Koster Van Groos 1991; Aranovich and Newton 1996).

The agreement between the experimental results and the calculated position of mineral–fluid equilibria is excellent, but it may be fortuitous because the effect of dissolved solutes other than NaCl was ignored. The solubility of the assemblage paragonite + kyanite + jadeite in H_2O ± NaCl is not known. However, experimental investigations of the solubility of albite and albite + quartz in H_2O ± NaCl at high P (Lin and Manning 2001; Stalder et al. 2000; Shmulovich et al. 2001; Antignano and Manning 2003) can be used as a guide to show that the expected effect of dissolved solutes on $a(H_2O)$ is negligible.

Studies of the solubility of albite in H_2O show that, at fixed P and T, dissolved solute concentration decreases with increasing bulk Al_2O_3/SiO_2, such that the solubility of albite + quartz is greater than albite alone (Antignano and Manning 2003). Solubility of albite in H_2O increases strongly with P at 600–700°C as the second critical end point is approached (Stalder et al. 2000); however, this effect is suppressed in peraluminous bulk compositions such as those of the present study. Stalder et al. (2000) found that albite + nepheline + $Al(OH)_3$ total solubility is 2.8 ± 1 wt% at 0.5 GPa, 725°C, and dissolved silicate is approximately

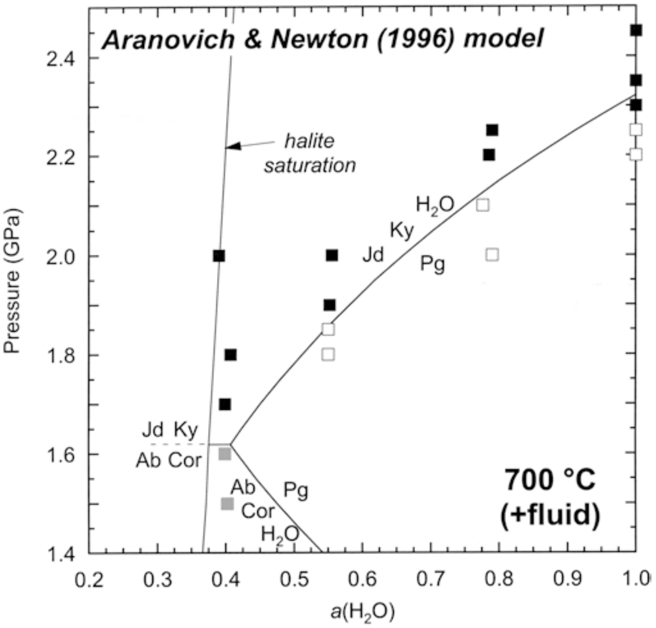

Fig. 5 P–$a(H_2O)$ diagram showing the position of the experimental data, where $a(H_2O)$ is calculated with the H_2O–NaCl activity model of Aranovich and Newton (1996). Reactions 1, 2, 3 were calculated with the program THERMOCALC v. 3.21 with the thermodynamic data base of Holland and Powell (1998). The *dashed line* indicates the position of the halite saturation curve, based on an extrapolation of the data of Koster Van Groos (1991) and Aranovich and Newton (1996). The width and height of the boxes corresponds to 1σ uncertainties in pressure and activity. The uncertainties in the calculated activities of ±0.01 are from Aranovich and Newton (1996)

albite in stoichiometry. Recent experimental studies indicate significant polymerization of solute Al and Si through formation of bridging oxygens (Manning 2004b). Hence, for the purposes of examining the effects of dissolved solutes on $a(H_2O)$, we may assume an average solute stoichiometry of $NaAlSi_3O_3(OH)_{10}$. Allowing conservatively for up to 20 wt% solute in H_2O at the conditions of our experiments, we calculate that the maximum H_2O added to the experiments (~2 mg, Table 1) would contain 1.91 μmol $NaAlSi_3O_3(OH)_{10}$. Formation of hydroxyls would transfer five times this quantity, or 9.55 μmol, H_2O from the bulk solvent to the solute molecule (this is a maximum since some H_2O would be liberated by paragonite hydrolysis). The solute-bearing solution would therefore have $X(H_2O) = 0.982$, which, assuming $a(H_2O) = X(H_2O)$, would lead to a reduction of $a(H_2O)$ by solutes by a maximum 0.018 in the NaCl-free system. This would correspond to a shift in reaction 1 to lower P by 0.013 GPa, which is the same as the P uncertainty in the experiments. NaCl addition is likely to reduce bulk albite solubility (Shmulovich et al. 2001), which would lead to progressively smaller effects of solutes on $a(H_2O)$ with increasing X(NaCl). It can therefore be concluded that our results are not affected by dissolved solutes.

Petrological implications

Due to their restricted bulk composition, jadeite + kyanite-bearing rocks very rarely occur in eclogite-facies metagranites or metapelites and hence the assemblage jadeite + kyanite has been described only from a few locations in the Western Alps (Monte Mucrone: Dal Piaz et al. 1972; Compagnoni and Maffeo 1973; Dora Maira: Chopin 1984; Biino and Compagnoni 1992; Compagnoni et al. 1995; Allalin metagabbro: Meyer 1983; Wayte et al. 1989). In addition to these localities, Barbero (1992), Venturini et al. (1994) and Tropper et al. (1999) described a partial transformation from a pre-Alpine igneous assemblage to an Eo-Alpine high-pressure assemblage in metapelites from Val Savenca. The metapelites of Val Savenca occur in the Polymetamorphic Basement Complex of the Sesia-Lanzo Zone and were metamorphosed during the Eo-Alpine event (Rubatto et al. 1999). The metapelites now contain an assemblage (K-feldspar + jadeite + zoisite + phengite + quartz ± kyanite) that replaced igneous and metamorphic plagioclase, along with garnet coronas around relict igneous or metamorphic titanian biotite (Barbero 1992; Venturini et al. 1994). Because of the partial transformation, only local equilibrium has been achieved leading to the formation of microdomains (Fig. 6a). Plagioclase is replaced by jadeite + zoisite + kyanite + quartz (Fig. 6b). Within the jadeite + zoisite + kyanite + K-feldspar pseudomorphs after plagioclase, jadeite and quartz coexist with K-feldspar (Fig. 6a, b). Biotite is replaced by the assemblage of phengite + omphacite + kyanite if it is adjacent to former plagioclase (Fig. 6A), otherwise by phengite + rutile/titanite, or only by phengite. Direct determination of pressures in eclogites in combination with temperature estimates make it possible to constrain $a(H_2O)$ for the partially equilibrated samples from Val Savenca with the assemblage jadeite + kyanite. $a(H_2O)$ has been evaluated by contouring a P–T diagram with $a(H_2O)$-isopleths for reaction 1. The P–T conditions were obtained by Tropper et al. (1999) by using garnet–clinopyroxene geothermometry and K-feldspar-jadeite-quartz geobarometry and yield 550–650°C and 1.7–2.0 GPa (Fig. 7). Since paragonite is absent this provides a *lower* limit for $a(H_2O)$ in the P–T space (Fig. 7). The obtained $a(H_2O)$ is low and ranges from 0.3 to 0.6 for the partially re-equilibrated samples from Val Savenca. Although no fluid inclusion studies exist from jadeite + kyanite-bearing rocks, lowering $a(H_2O)$ could be due to the presence of saline brines, which have been described from numerous high pressure rocks of the Western Alps (Philippott and Selverstone 1991; Nadeau et al. 1993; Scambelluri and Philippot 2001).

Based on petrographical and mineral chemical investigations in eclogites from the Sesia Lanzo Zone, Tropper and Essene (2002) were able to show that the occurrence of paragonite as an inclusion in the core of a garnet serves as a monitor for changing $a(H_2O)$ conditions. Paragonite occurs as inclusion in the garnet core

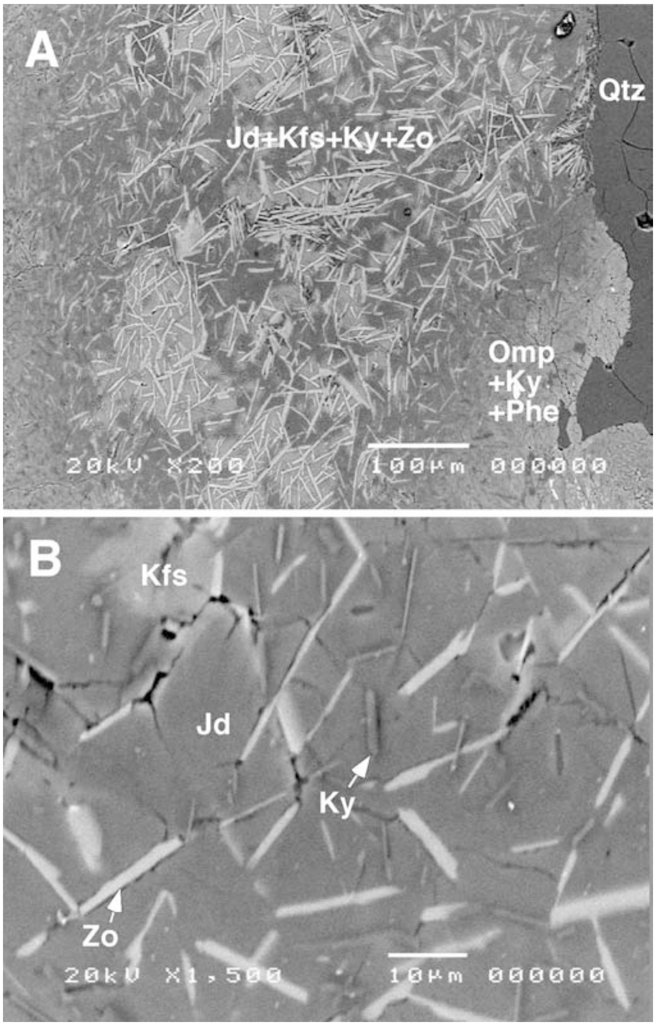

Fig. 6a, b BSE images of the partially transformed metapelites from Val Savenca (Sesia Zone, Italy, sample VS-8). **a** Overview over a former plagioclase site, where Pre-Alpine plagioclase is now replaced by the Eo-Alpine eclogite-facies assemblage jadeite (Jd) + K-feldspar (Kfs) + kyanite (Ky) + zoisite (Zo). In the lower right, at the border to a former biotite, the assemblage omphacite (Omp) + Kyanite (Ky) + phengite (Phe) forms. **b** Close-up of the assemblage (Jd) + K-feldspar (Kfs) + kyanite (Ky) + zoisite (Zo) from the center of the plagioclase domain

and disappears towards the rims of the garnet porphyroblasts and the assemblage omphacite + kyanite forms instead. Whereas in the matrix, the assemblage paragonite + omphacite is present and kyanite is absent. Since there is no chemical evidence in the garnet zoning (e.g. changing pyrope and grossular contents), indicating neither an increase in temperature nor in pressure which occurred coeval with the disappearance of paragonite and the formation of omphacite + kyanite, changing $a(H_2O)$ might be responsible for the mineralogical changes. These changes can be explained with a decrease in $a(H_2O)$ from ca. 1.0 to 0.39–0.81 while the garnet grew, thus stabilizing the assemblage omphacite + kyanite instead of paragonite. During the subsequent hydration in the late eclogite-facies, the pressure dropped slightly indicated by lower grossular contents in the outermost garnet rims and $a(H_2O)$ seemed to have increased (0.84–0.98). Therefore the assemblage paragonite + omphacite forms again.

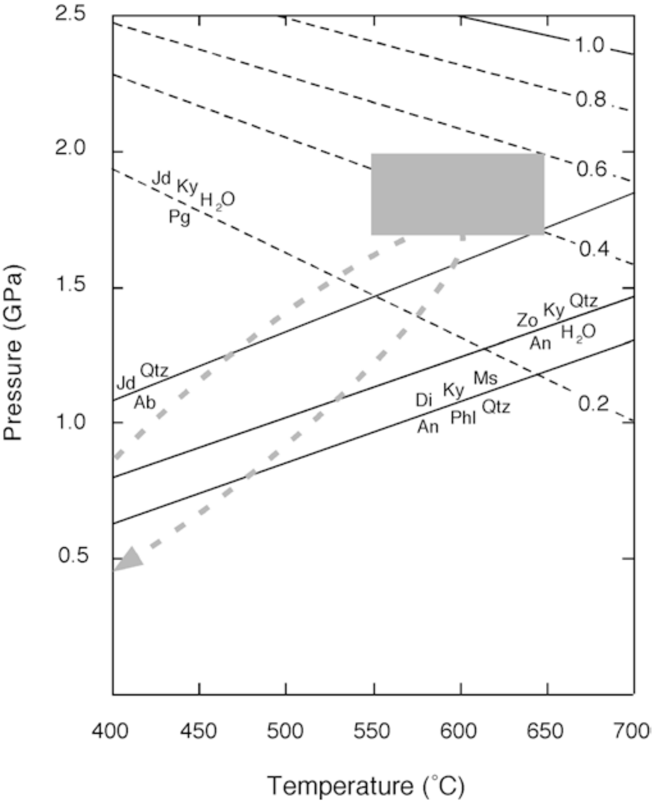

Fig. 7 *P–T* $a(H_2O)$ estimates from the eclogite-facies metapelites from Val Savenca obtained with K-feldspar-jadeite-quartz geobarometry and garnet-clinopyroxene thermometry (Tropper et al. 1999) as shown in the grey box and estimation of $a(H_2O)$ limits for the assemblage jadeite + kyanite from the partially re-equilibrated metapelites. The estimation of $a(H_2O)$ is based on reaction 1 and the *numbers* on the *right side* of the diagram represent values of constant $a(H_2O)$ along each curve ($a(H_2O) = 1$; *solid line*, $a(H_2O) < 1$; *dashed lines*). Based on image analysis, the composition of the precursor plagioclase was estimated to be $Ab_{70}An_{30}$ and relevant equilibria involving protolith plagioclase and biotite, such as albite = jadeite + quartz, anorthite + H_2O = zoisite + kyanite + quartz and anorthite + phlogopite + quartz = diopside + kyanite + muscovite, were calculated with THERMOCALC v. 3.21. For comparison the *P–T* path from Venturini 1995) is also shown. All mineral abbreviations are according to Kretz (1983)

The experiments thus provide very useful limiting information on $a(H_2O)$ of fluids on the H_2O–NaCl binary coexisting either with paragonite or the assemblage jadeite + kyanite in eclogite-facies rocks. Based on the experimental constraints, paragonite + jadeite (omphacite) + kyanite-bearing rocks have great potential in providing at least limiting estimates for $a(H_2O)$ of a fluid phase coexisting with this assemblage if one independent variable (*P* or *T*) is known and an appropriate activity model for omphacite solid solutions is used.

Acknowledgements This work was supported by NSF grants EAR 9909583 and 0337170 to CEM. Angelo Antignano IV and Robert

Newton are thanked for their help in the UCLA piston-cylinder laboratory. Karl Ettinger is thanked for his help with the SEM at the Institute of Mineralogy and Petrology, University of Graz. The constructive reviews of Tim Holland and Hans Keppler and the editorial handling of Werner Schreyer are greatly appreciated.

References

Antignano A IV, Manning CE (2003) Solubility of albite + paragonite ± quartz in H_2O at 1 GPa, 580°C: implications for metamorphic fluids. Eos Trans AGU, 84(46), Fall Meet Suppl, Abstract V22D-0613, 2003

Aranovich LY, Newton RC (1996) H_2O activity in concentrated NaCl solutions at high pressures and temperatures measured by the brucite-periclase equilibrium. Contrib Miner Petrol 125:200–212

Aranovich LY, Newton RC (1997) H_2O activity in concentrated KaCl and KCl–NaCl solutions at high temperatures and pressures measured by the brucite-periclase equilibrium. Contrib Miner Petrol 127:261–271

Aranovich LY, Newton RC (1998) Reversed determination of the reaction: phlogopite + quartz = enstatite + potassium feldspar + H_2O in the ranges 750–875°C and 2–12 kbar at low H_2O activity with concentrated KCl solutions. Am Miner 83:193–204

Barbero M (1992) Geologia dell'alto vallone del Savenca (Zona Sesia-Lanzo, Alpi Occidentali). MSc Thesis, University of Torino

Berman RG (1988) Internally-consistent thermodynamic data for minerals in the system Na_2O–K_2O–CaO–FeO–Fe_2O_3–Al_2O_3–SiO_2– TiO_2–H_2O–CO_2. J Petrol 29:445–522

Biino GG, Compagnoni R (1992) Very-high pressure metamorphism of the Brossasco coronite metagranite, southern Dora Maira Massif, Western Alps. Schweiz Miner Petrol Mitt 72:347–363

Bohlen SR (1984) Equilibria for precise pressure calibration and a frictionless furnace assembly for the piston-cylinder apparatus. N Jb Miner Monatshefte 9:404–412

Bohlen SR, Montana AL, Kerrick DM (1991) Precise determination of the equilibria kyanite—sillimanite and kyanite– andalusite and a revised triple point for Al_2SiO_5 polymorphs. Am Miner 76:677–680

Boyd FR, England JL (1960) Apparatus for phase equilibrium measurements at pressures up to 50 kilobars and temperatures up to 1750°C. J Geophys Res 65:741–748

Chopin C (1984) Coesite and pure pyrope in high-grade blueschists of the western Alps: a first record and some consequences. Contrib Miner Petrol 86:107–118

Compagnoni R, Maffeo B (1973) Jadeite-bearing metagranites l.s. and related rocks in Monte Mucrone area (Sesia-Lanzo Zone, Western Italian Alps). Schweiz Miner Petrogr Mitt 53:355–378

Compagnoni R, Hirajima T, Chopin C (1995) Ultra-high pressure metamorphic rocks in the Western Alps. In: Coleman RG, Wang X (eds) Ultrahigh pressure metamorphism. Cambridge University Press, New York, pp 206–244

Dal Piaz GV, Hunziker JC, Martinotti G (1972) La Zona Sesia-Lanzo e l'evoluzione tectonico-metamorphica della Alpi nord-occidentali interne. Mem Soc Geol Ital 11:433–466

Fryer P, Pearce JA, Stokking LB et al (1990) Proc ODP Init Repts 125, College Station TX, p 1092

Gao J, Klemd R (2001) Primary fluids entrapped at blueschist to eclogite transition: evidence from the Tianshan meta-subduction complex in northwest China. Contrib Miner Petrol 142:1–14

Giaramita MJ, Sorensen SS (1994) Primary fluids in low-temperature eclogites: evidence from two subduction complexes (Dominican Republic, and California, USA). Contrib Miner Petrol 117:279–292

Haar L, Gallagher JS, Kell GS (1984) NBS/NRC steam tables. Hemisphere, New York, p 320

Holland TJB (1979) Experimental determination of the reaction paragonite = jadeite + kyanite + H_2O, and internally consistent thermodynamic data for part of the system Na_2O–Al_2O_3–SiO_2–H_2O, with applications to eclogites and blueschists. Contrib Miner Petrol 68:293–301

Holland TJB, Powell R (1991) A compensated-Redlich-Kwong (CORK) equation for volumes and fugacities of CO_2 and H_2O in the range 1 bar to 50 kbar and 100–1600°C. Contrib Mineral Petrol 109:265–273

Holland TJB, Powell R (1998) An internally-consistent thermodynamic data set for phases of petrological interest. J Metam Geol 8:89–124

Iwamori H (1998) Transportation of H_2O and melting in subduction zones. Earth Planet Sci Lett 160:65–80

Jarrad RD (2003) Subduction fluxes of water, CO_2, chlorine, and potassium. Geochim Geophys Geosys.DOI:10.1029/2002GC000392

Johnson JW, Oelkers EH, Helgeson HC (1992) SUPCRT92; a software package for calculating the standard nolal thermodynamic properties of minerals, gases, aqueous species, and reactions from 1 to 5000 bar and 0 to 1000°C. Comp Geosci 18:899–947

Keppler H (1996) Constraints from partitioning experiments on the composition of subduction-zone fluids. Nature 380:237–240

Kimura G, Silver E, Blum P et al (1997) Proc ODP Init Repts 170, College Station TX, p 458

Koster Van Groos AF (1991) Differential thermal analysis of the liquidus relations in the system NaCl-H_2O to 6 kbar. Geochim Cosmochim Acta 55:2811–2817

Kretz R (1983) Symbols for rock-forming minerals. Am Miner 68:277–279

Lin H, Manning CE (2001) Albite–paragonite–quartz solubility: experimental constraints on the thermodynamic behavior of Si, Al, and Na in aqueous fluids at 0.5–1.0 GPa from 350–500°C. EOS Trans AGU Fall Meet Suppl 82:V32B–0969

Manning CE (1994) The solubility of quartz in H_2O in the lower crust and upper mantle. Geochim Cosmochim Acta 58:4831–4839

Manning CE (2004a) The chemistry of subduction-zone fluids. Earth Planet Sci Lett (in press)

Manning CE (2004b) Polymeric silicate complexing in aqueous fluids at high pressure and temperature, and its implications for water-rock interaction. WRI-11, Abstract (in press)

Manning E, Boettcher SL (1994) Rapid-quench hydrothermal experiments at mantle pressures and temperatures. Am Miner 79:1153–1158

Meyer J (1983) The development of the high pressure metamorphism in the Allalin metagabbro (Switzerland). Terra Cognita 3:187

Nadeau S, Philippot P, Pineau F (1993) Fluid inclusion and mineral isotopic compositions (H-C-O) in eclogitic rocks as tracers of local fluid migration during high-pressure metamorphism. Earth Planet Sci Lett 114:431–448

Newton RC, Manning CE (2000) Quartz solubility in H_2O–NaCl and H_2O–CO_2 solutions at deep crust-upper mantle pressures and temperatures: 2–15 kbar and 500–900°C. Geochim Cosmochim Acta 64:2993–3005

Newton RC, Manning CE (2002) Experimental determination of calcite solubility in H_2O–NaCl solutions at deep crust/upper mantle pressures and temperatures: implications for metasomatic processes in shear zones. Am Miner 87:1401–1409

Newton RC, Manning CE (2004) Solubility of anhydrite, $CaSO_4$, in NaCl–H_2O solutions at high pressures and temperatures: applications to fluid-rock interaction. J Petrol (submitted)

Philippot P (1993) Fluid-melt-rock interaction in mafic eclogites and coesite-bearing metasediments: constraints on volatile recycling during subduction. Chem Geol 108:93–112

Philippot P, Selverstone J (1991) Trace element-rich brines in eclogitic veins: implications for fluid compositions and transport during subduction. Contrib Miner Petrol 106:417–430

Rubatto D, Gebauer D, Compagnoni R (1999) Dating of eclogite-facies zircons: the age of Alpine metamorphism in the Sesia-Lanzo Zone (Western Alps). Earth Planet Sci Lett 167:141–158

Sadovsky S, Bebout GE (2003) Record of forearc devolatilization in low-*T*, high *P*/*T* metasedimentary suites: significance for models of convergent margin chemical cycling. Geochem Geophys Geosys 4:29

Scambelluri M, Philippot P (2001) Deep fluids in subduction zones. Lithos 55:213–227

Schmidt MW, Poli S (1998) Experimentally based water budgets for dehydrating slabs and consequences for arc magma generation. Earth Planet Sci Lett 163:361–379

Selverstone J, Franz G, Thomas S, Getty S (1992) Fluid variability in 2 GPa eclogites as an indicator of fluid behavior during subduction. Contrib Mineral Petrol 112:314–357

Shmulovich K, Graham C, Yardley BWD (2001) Quartz, albite and diopside solubilities in H_2O–NaCl and H_2O–CO_2 fluids at 0.5–0.9 GPa. Contrib Miner Petrol 141:95–108

Stalder R, Ulmer P, Thompson AB, Günther D (2000) Experimental approach to constrain second critical end points in fluid/silicate systems: near-solidus fluids and melts in the system albite-H_2O. Am Miner 85:68–77

Stern RJ (2002) Subduction zones. Rev Geophys 40:3–38

Thomas S (1991) Zur Kluftbildung in Gesteinen der Eklogitzone (Hohe Tauern, Österreich). Unpublished PhD Thesis, Technical University

Touret JLR (2001) Fluids in metamorphic rocks. Lithos 55:1–25

Tropper P, Essene EJ (2002) Thermobarometry in eclogites with multiple stages of mineral growth: an example from the Sesia-Lanzo Zone (Western Alps, Italy). Schweiz Miner Petrogr Mitt 82:487–514

Tropper P, Essene EJ, Sharp ZD, Hunziker JC (1999) Application of K-feldspar-jadeite-quartz barometry to eclogite facies metagranites and metapelites in the Sesia Lanzo Zone (Western Alps, Italy). J Metam Geol 17:195–209

Ulmer P (2001) Partial melting in the mantle wedge—the role of H_2O in the genesis of mantle-derived "arc-related" magmas. Phys Earth Planet Int 127:215–232

Venturini G, Martinotti G, Armando G, Barbero M, Hunziker JC (1994) The Central Sesia-Lanzo Zone (Western Italian Alps): new field observations and lithostratigraphic subdivisions. Schweiz Mineral Petrograph Mitt 74:111–121

Wayte GJ, Worden RH, Rubie DC, Droop GTR (1989) A TEM study of disequilibrium plagioclase breakdown at high pressure: the role of infiltrating fluid. Contrib Miner Petrol 101:426–437

Yardley BWD, Graham JT (2002) The origins of salinity in metamorphic fluids. Geofluids 2:249–256